

Electronic Interactions in Verdazyl Biradicals

Rosario M. Fico Jr., Michael F. Hay, Scott Reese, Steve Hammond, Elizabeth Lambert, and Marye Anne Fox*

Department of Chemistry and Biochemistry, University of Texas at Austin, Austin, Texas 78712, and Department of Chemistry North Carolina State University, Raleigh, North Carolina 27675

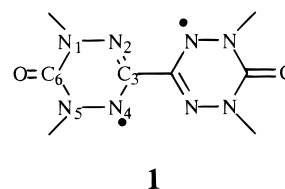
Received June 15, 1999

A series of bisverdazyl biradicals in which the atoms bearing the greatest spin density are separated by several different aromatic spacer groups has been prepared in order to compare their properties to those of the nonspaced 1,1',5,5'-tetramethyl-6,6'-dioxo-3,3'-bisverdazyl (**1**). In addition, the 6,6'-dithio derivative (1,1',5,5'-tetramethyl-6,6'-dithio-3,3'-bisverdazyl (**7**)) was prepared. Cyclic voltammograms of 1,4-bis(1,5-dimethyl-6-oxo-3-verdazyl)benzene (**5**) and 2,5-bis(1,5-dimethyl-6-oxo-3-verdazyl)thiophene (**6**) both show a single two-electron oxidation near 700 mV. In contrast **1**, **7**, and 1,3-bis(1,5-dimethyl-6-oxo-3-verdazyl)benzene (**4**) display two one-electron oxidation waves, with the first oxidative wave appearing also near 700 mV. The absorption spectrum of each of these biradicals was red-shifted from the maximum observed for **1**. Biradicals **4**, **5**, and **6** exhibited linear Curie plots, although a curved Curie plot was observed for **7** with $J = 560 \text{ cm}^{-1}$.

Introduction

There has been recent interest in the development and study of the magnetic properties of stable organic radicals and polyradicals.^{1–7} Radicals can act as electron donors or acceptors, can ligate to metals, and can act as redox-active centers.^{8–13} These are desirable properties for the development of molecular wires and molecular based magnetic materials. Organic materials are anticipated to be easily processible, lightweight, soluble in organic solvents, and/or optically transparent. It is hoped that by employing common organic synthetic techniques, these molecules may be “tuned” to have the desired properties.

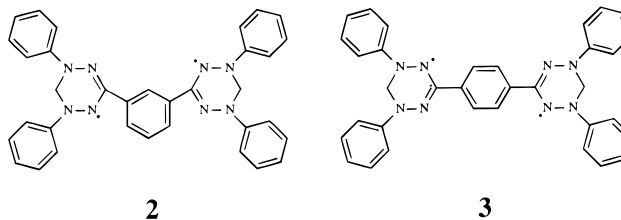
To this end we have investigated a stable biradical, 1,1',5,5'-tetramethyl-6,6'-dioxo-3,3'-bisverdazyl (**1**), a compound first prepared by Neugebauer and Fischer and closely related to the monoverdazyl radicals studied by Kuhn and Trischman.^{14–16}



1

Bisverdazyl biradical **1**, a stable biradical whose HOMO and LUMO are very similar to those of tetramethylethane (TME),^{10,17} can be thought of as a heterocyclic analogue to TME. Previous Hückel MO-LCAO calculations of verdazyl biradicals have indicated that the unpaired electrons reside in degenerate molecular orbitals and the electron density at C₃ is very near zero.¹⁸ Verdazyls are generally stable compounds that can be easily handled in the lab and are synthetically adaptable to a wide variety of substituents.

The electronic interactions in **1** were studied previously by this group.¹⁰ Bisverdazyl **1** is a non-Kekulé disjoint biradical, existing as a ground state singlet with small contributions of a thermally populated triplet. The spaced compounds **2** and **3** exist as ground-state triplets with a zero field splitting parameter, D , of 0.0050 and 0.0040 cm^{-1} , respectively.^{19,20}



2

3

(1) Miller, J. S.; Epstein, A. J. *Angew. Chem., Int. Ed. Engl.* **1994**, *33*, 385.

(2) Borden, W. T.; Iwamura, H.; Berson, J. A. *Acc. Chem. Res.* **1994**, *27*, 109.

(3) Dougherty, D. A. *Acc. Chem. Res.* **1991**, *24*, 88.

(4) Rajca, A. *Chem. Rev.* **1994**, *94*, 871.

(5) Miller, J. S.; Epstein, A. J.; Reiff, W. M. *Chem. Rev.* **1988**, *88*, 201.

(6) Caneschi, A.; Gatteschi, D.; Sessoli, R.; Rey, P. *Acc. Chem. Res.* **1989**, *22*, 392.

(7) Iwamura, H.; Koga, N. *Acc. Chem. Res.* **1993**, *26*, 346.

(8) Bryan, C. D.; Cordes, A. W.; Goddard, J. D.; Haddon, R. C.; Hicks, R. G.; MacKinnon, C. D.; Mawhinney, R. C.; Oakley, R. T.; Palstra, T. T. M.; Perel, A. S. *J. Am. Chem. Soc.* **1996**, *118*, 330.

(9) Barclay, T. M.; Cordes, A. W.; de Laat, R. H.; Goddard, J. D.; Haddon, R. C.; Jeter, D. Y.; Mawhinney, R. C.; Oakley, R. T.; Palstra, T. T. M.; Patenaude, G. W.; Reed, R. W.; Westwood, N. P. C. *J. Am. Chem. Soc.* **1997**, *119*, 2633.

(10) Brook, D. J. R.; Fox, H. H.; Lynch, V.; Fox, M. A. *J. Phys. Chem.* **1996**, *100*, 2066.

(11) Brook, D. J. R.; Lynch, V.; Conklin, B.; Fox, M. A. *J. Am. Chem. Soc.* **1996**, *119*, 5155.

(12) Inoue, K.; Iwamura, H. *Angew. Chem., Int. Ed. Engl.* **1995**, *34*, 927.

(13) Luneau, D.; Laugier, J.; Rey, P.; Ulrich, B.; Ziessel, R.; Legoll, P.; Drillon, M. *J. Chem. Soc., Chem. Commun.* **1994**, 741.

(14) Neugebauer, F. A.; Fischer, H. *Angew. Chem., Int. Ed. Engl.* **1980**, *19*, 724.

(15) Kuhn, R.; Trischmann, H. *Angew. Chem., Int. Ed. Engl.* **1963**, *2*, 155.

(16) Kuhn, R.; Neugebauer, F. A.; Trischmann, H. *Angew. Chem., Int. Ed. Engl.* **1964**, *3*, 232.

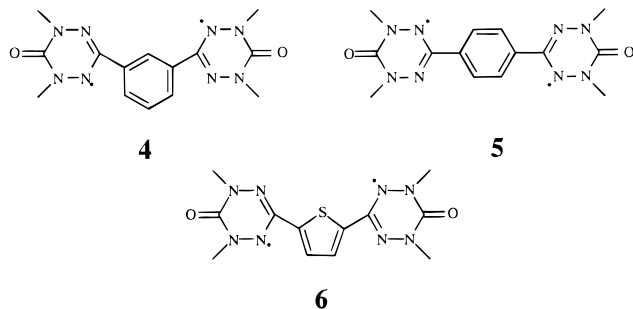
(17) Borden, W. T.; Davidson, E. R. *J. Am. Chem. Soc.* **1977**, *99*, 4587.

(18) Fischer, H. H. *Tetrahedron* **1967**, *23*, 1939.

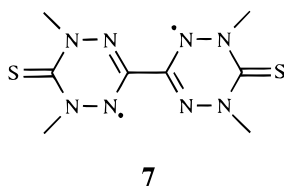
(19) Mukai, K.; Azuma, N.; Shikata, H.; Ishizu, K. *Bull. Chem. Soc. Jpn.* **1970**, *43*, 3958.

(20) Azuma, N.; Ishizu, K.; Mukai, K. *J. Chem. Phys.* **1974**, *61*, 2294.

This difference in multiplicity prompted us to study the effects of the intervening spacer group on the electronic characteristics of a series of bisverdazyl biradicals. To this end, with **1** as the parent compound, three bisverdazyls with aromatic spacer units were synthesized: 1,3-bis(1,5-dimethyl-6-oxo-3-verdazyl)benzene (**4**), 1,4-bis(1,5-dimethyl-6-oxo-3-verdazyl)benzene (**5**), and 2,5-bis(1,5-dimethyl-6-oxo-3-verdazyl)thiophene (**6**).



Furthermore, we were able to observe the variation in electron density in the π framework by substituting the oxygen in **1** for the more electronegative sulfur as in 1,1',5,5'-tetramethyl-6,6'-dithio-3,3'-bisverdazyl (**7**).



To fully understand the intramolecular interactions within this series, we have investigated the electrochemical properties and the absorption and electron spin resonance spectra of these biradicals.

Results and Discussion

Synthesis and Properties of 4–7. Biradicals **4–6** were synthesized by condensing isophthalaldehyde, terephthalaldehyde, or 2,5-thiophenedicarboxaldehyde with 2,4-dimethyl carbonohydrazide. Oxidations to the neutral biradical were carried out with potassium ferricyanide for the electrochemical and absorption experiments and with lead oxide or tetraphenylhydrazine for the EPR experiments. The thio analogue **7** was similarly prepared from the thiohydrazide. Compounds **4–6** were sufficiently stable to be characterized by chemical ionization high-resolution mass spectra analysis, but compound **7** proved to be too air sensitive for MS analysis and was characterized by other in situ spectral methods.

Room-temperature electron paramagnetic resonance (EPR) spectra of the spaced biradicals **4–7** are similar to that of **1** within our experimental determination. Linear Curie plots were observed for **4–7**, indicating either a ground state triplet or nearly degenerate singlet/triplet energy levels.²¹ However, the absorption spectra of **4–7** are red-shifted compared with **1**. Electrochemical measurements show that the stability of the dications and dianions derived from these biradicals are also sensitive to structural variation.

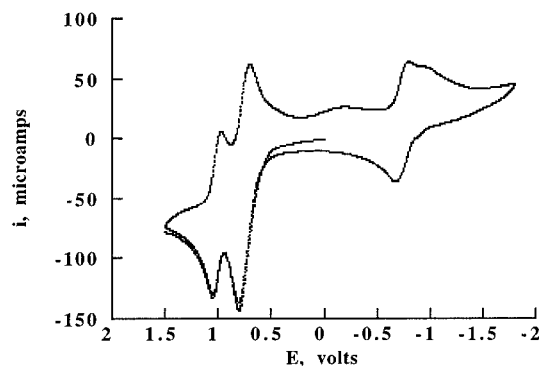


Figure 1. Cyclic voltammetric scan on Pt wire of 1.0 mM **1** in degassed CH_3CN containing 0.1 M NBu_4PF_6 . Scan rate: 250 mV/s.

The room-temperature EPR spectrum of **7** is also almost identical to that of **1**. The observation of a triplet spectrum in frozen chloroform, however, reveals zero-field splitting parameters (z_{fp}) and substantial changes in electron density and molecular symmetry. The absorption spectrum of **7** is also red-shifted, and electrochemical measurements indicate the thio analogue to be less stable and more easily oxidized and reduced than **1**.

Electrochemical Behavior. Despite the many EPR studies of verdazyls, very few substituted verdazyls have been studied electrochemically.^{10,14,15,22–29} The available literature reports have focused on the electrochemistry of 1,3,5-triphenylverdazyl in determining the effect of solvent on reaction entropies and disproportionation equilibria.^{30,31} Oxidation of 1,3,5-triphenylverdazyl to the cation was reported to be reversible, but the reduction to the anion is only quasireversible.^{30,31} $E_{1/2}$ potentials were not stated, but the peak separation between the anodic and cathodic peaks was given as $\Delta E_{\text{p}^{\text{ox}}} = 60$ mV and $\Delta E_{\text{p}^{\text{red}}} = 110$ mV, respectively.^{30,31} It is likely that the stability of the mono and dications of **1** and of **4–7** are related to the stability of the analogous cations.

Cyclic voltammetry of **1**, **7**, and **4** in degassed acetonitrile solutions shows substantially different electrochemical behavior. In **1**, two quasireversible oxidation waves are seen as the neutral biradical is first converted to a radical cation (803 mV) and then to a dication (1.05 V) (Figure 1). In the reduction, one two-electron wave is observed as the molecule goes from the neutral biradical to the dianion. In **7**, two one-electron oxidation waves are also seen (778 mV, 902 mV), only one of which is reversible (Figure 2). The return reduction wave of **7** is suppressed, indicating that the two-electron reduction is

(22) Katritzky, A. R.; Belyakov, S. A.; Durst, H. D.; Xu, R.; Dalal, N. S. *Can. J. Chem.* **1994**, *72*, 1849.

(23) Neugebauer, F. A. *Angew. Chem., Internat. Ed. Engl.* **1973**, *12*, 455.

(24) Kuhn, R.; Neugebauer, F. A.; Trischmann, H. *Monatsh.* **1966**, *97*, 525.

(25) Neugebauer, F. A. *Tetrahedron* **1970**, *26*, 4853.

(26) Dormann, E.; Winter, H.; Dyakonow, W.; Gotschy, B.; Lang, A.; Naarmann, H.; Walker, N. *Ber. Bunsen-Ges. Phys. Chem.* **1992**, *96*, 922.

(27) Neugebauer, F. A.; Fischer, H.; Krieger, C. *J. Chem. Soc., Perkin Trans. 2* **1993**, 535.

(28) Neugebauer, F. A.; Fischer, H.; Siegel, R. *Chem. Ber.* **1988**, *121*, 815.

(29) Neugebauer, F. A.; Fischer, H.; Krieger, C. *Chem. Ber.* **1983**, *116*, 3461.

(30) Jaworski, J. S. *Electroanal. Chem.* **1991**, *300*, 167.

(31) Jaworski, J. S.; Krawczyk, I. *Monatsh. Chem.* **1992**, *123*, 43.

(21) Berson, J. A. *The Chemistry of the Quinonoid Compounds*; Wiley: New York, 1988; Vol. 2, Chapter 10.

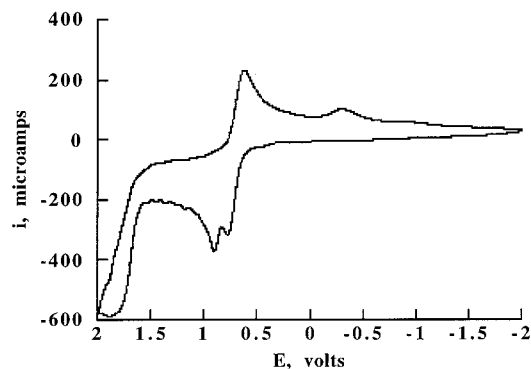


Figure 2. Cyclic voltammogram on Pt wire of 1.0 mM **7** in degassed CH₃CN containing 0.1 M NBu₄PF₆. Scan rate: 1000 mV/s.

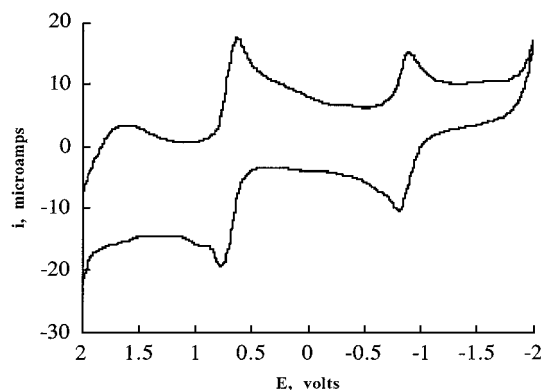


Figure 3. Cyclic voltammogram on Pt wire of 1.0 mM **4** in degassed CH₃CN containing 0.1 M NBu₄PF₆. Scan rate: 1000 mV/s.

Table 1. Electrochemical Data for Verdazyl Biradicals (mV vs SCE)

	$E_{1/2}$ (0/+)	ΔE_p	$E_{1/2}$ (•+/2+)	ΔE_p	$E_{1/2}$ (0/•-)	ΔE_p	Δ_{ox} (mV)
1	755	93	1013	75	-728	105	248
7	701	152	763	275	-304	irr.	123
4	706	144	814	360	849	79	216
	$E_{1/2}$ (0/2+)	ΔE_p	$E_{1/2}$ (0/2-)	ΔE_p			
5	685	134	-800	>200			
6	749	155	-815	130			

not reversible. As with **1** and **7**, **4** also displays two one-electron oxidation waves (778, 994 mV) (Figure 3). In the reduction, however, only one two-electron wave is observed. As indicated in Table 1, the difference between the first one-electron oxidation wave and the second one-electron oxidation wave, Δ_{ox} , is twice as large in **1** as in **7**. This suggests that there is greater interaction between the two unpaired electrons in **1** than in **7**.

In the spaced biradicals **5** (Figure 4) and **6** (Figure 5), cyclic voltammetry shows one two-electron reduction wave and one two-electron oxidation wave, rather than the two one-electron oxidation waves as observed in **1**, **4**, and **7**. These waves are found at approximately the same potentials in these biradicals (Table 1). This indicates that there is less communication between the two unpaired electrons in **5** and **6** than in **1**.

In all of these systems, the peak separation between the forward and reverse scans of the reduction waves is larger than that for the oxidation waves (Table 1), further

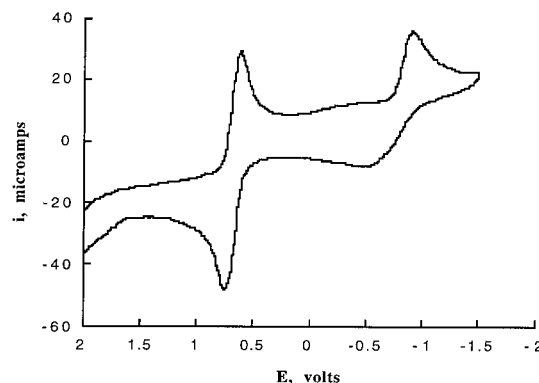


Figure 4. Cyclic voltammogram on Pt wire of 1.0 mM **5** in degassed CH₃CN containing 0.1 M NBu₄PF₆. Scan rate: 1000 mV/s.

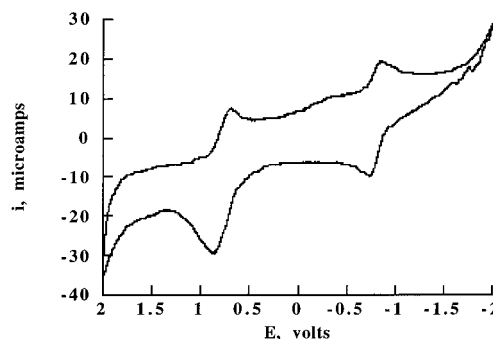


Figure 5. Cyclic voltammogram on Pt wire of 1.0 mM **6** in degassed CH₃CN containing 0.1 M NBu₄PF₆. Scan rate: 1000 mV/s.

indicating significant irreversibility in the dianion. Dianion instability is also shown by the suppression of the return reduction wave in **5**, indicating either unimolecular decomposition of the reduced product or its participation in a complicating side reaction.

Thus, cyclic voltammetry shows little coupling between radical centers in **5** and **6**, but substantial coupling in **1**, **4**, and **7**. As with the verdazyl monoradicals, the stability of the cations is greater than that of the anions, as revealed by the larger peak separation in the reduction and the suppression of the return reduction waves in **5** and **6**.

Absorption Spectroscopy. Each of the biradicals (**1**, **4**–**7**) is deeply colored, ranging from yellow to black. Simple MO calculations suggest that in the SOMO the bridging carbons are at nodal positions or that the electron density is close to zero at C₃.^{10,32} However, the absorption spectra of the spaced biradicals are all red-shifted from **1** (Figure 6), suggesting an increase in conjugation. In the LUMO, the bridging carbons are not at nodal positions and there would be considerable interaction between the verdazyl radical units and the spacer group. Indeed, from the spacer groups examined here, the degree of red shift follows the expected path of increased conjugation in the LUMO.

The meta-spaced bisverdazyl **4** is only red-shifted from **1** by 6 nm. *m*-Phenylene permits the least through- π interaction of the spacer groups examined. In **5**, whose connectivity is para through the phenyl spacer, the

(32) Forrester, A. R.; Hay, J. M.; Thomson, R. H. *Organic Chemistry of Stable Free Radicals*; Academic Press: London, 1968.

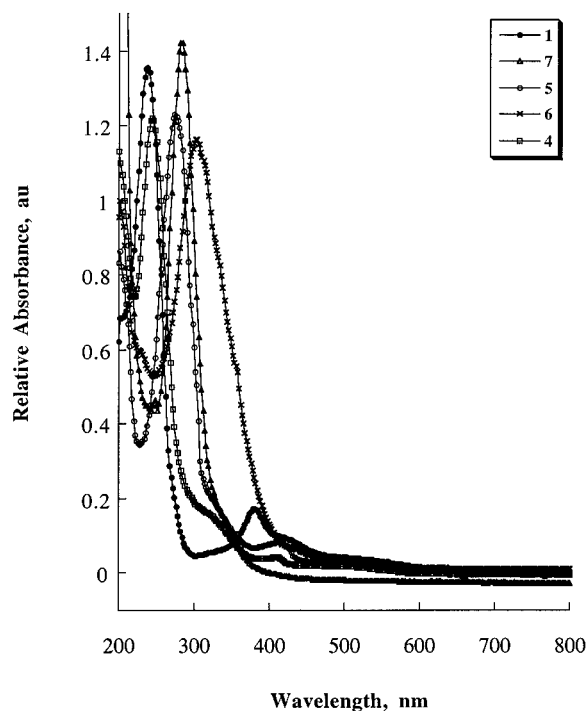


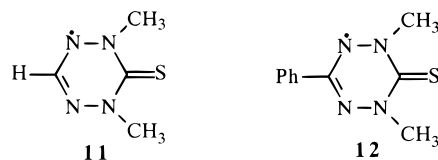
Figure 6. Absorption spectra of **1**, **4–7** in degassed acetonitrile solution.

absorption spectrum is red-shifted by 36 nm from **1**. The thiophene group in **6** shifts the absorption maximum by 66 nm from **1**. The thiophene group also broadens the spectrum of **6** considerably, giving rise to several shoulders on a broad peak, with a tail extending into the visible region. The long wavelength bands in **5** and **6** are particularly weak, indicating that although the addition of a thiophene or phenyl group provides some extension of the conjugated system, electronic transitions to this state are forbidden. The absorption spectrum of **7** (Figure 6) shows that the substitution of oxygen by sulfur at C₆ induces a red shift in the absorption maximum by 46 nm.²⁷ Noticeably absent are strong absorptions in the visible region.

These results can be best interpreted in relationship to the spectrum of the monoverdazyl radical. The absorption spectrum of monoverdazyls show two bands between 275 and 325 nm, two bands in the visible region from 400 to 450 nm, and one long wavelength band near 700 nm characteristic of $\pi-\pi^*$ transitions in highly conjugated chromophoric chains, as seen in 1,3,5-triphenylverdazyl.²² Bands in the visible region have previously been assigned to Φ_h (SOMO) \rightarrow Φ_1 (LUMO) and $\Phi_{h-1} \rightarrow \Phi_h$ (SOMO) transitions.²⁷

Using an analogous numbering system as in the bisverdazyls, substitution at C₃ greatly affects electronic structure, as reflected by changes in the absorption spectrum. A comparison of the absorption spectra of 1,5-dimethyl-6-thioverdazyl (**11**) with that of 1,5-dimethyl-3-phenyl-6-thioverdazyl (**12**) shows that a phenyl group at C₃ induces a red shift of approximately 30 nm from 276 to 303 nm and from 495 to 526 nm.²⁸

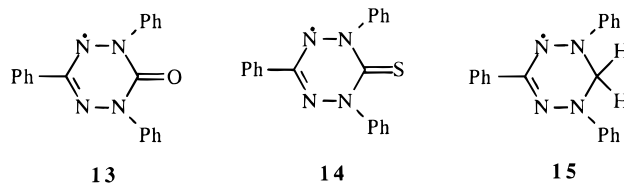
Substitution at C₆ also results in a significant shift, as seen in the substantial red shift induced by replacement of oxygen with sulfur at the C₆ position in 1,3,5-triphenyl-6-oxoverdazyl (**13**) and 1,3,5-triphenyl-6-thioverdazyl (**14**). Replacement of the sulfur with two C–H



$\lambda_{\max} = 276 \text{ nm and } 495 \text{ nm}$

$\lambda_{\max} = 303 \text{ nm and } 526 \text{ nm}$

bonds in **15** causes an even larger red shift of the long wavelength (by 50 nm).²⁷



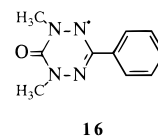
$\lambda_{\max} = 563 \text{ nm}$

$\lambda_{\max} = 608 \text{ nm}$

$\lambda_{\max} = 720 \text{ nm}$

Previous experimental and computational studies have shown that the substitution at N₁ and N₅ positions has little effect on the electronic structure of the verdazyl monoradical, unless the nitrogens participate in an extension of the conjugated π -system.¹⁸ Manipulation of substituents at N₁ and N₅ similarly results in only slight shifts of either the absorption spectrum or the chemical stability of the radical.²³ The similarity in spectral properties observed in biradicals **5** and **7** is therefore quite reasonable.

EPR Spectra. EPR spectra of chloroform solutions of **4–7** are similar to spectra reported previously for the phenyl-substituted monoverdazyl **16**.¹⁴



16

Solution spectra of **4–7** show at least nine lines with a 1:4:10:16:19:16:10:4:1 splitting pattern consistent with hyperfine coupling constants $A(N_{2,4}) \approx 6\text{--}5 \text{ Hz}$ and $A(N_{1,5}) \approx 5 \text{ Hz}$.²³ Smaller hyperfine coupling constants could not be determined due to large line widths and underlying monoradical impurities. These splitting patterns indicate the presence of four nitrogen atoms with nearly the same spin densities.¹⁸ The resolution of these spectra is considerably poorer than that of **16**, as is consistent with previous studies that show decreased resolution upon increasing the number of radical centers linked through a phenyl group.^{18,24} The observed line broadening was assigned to intermolecular hyperfine interactions and the intermolecular magnetic dipole–dipole interactions.^{18,26}

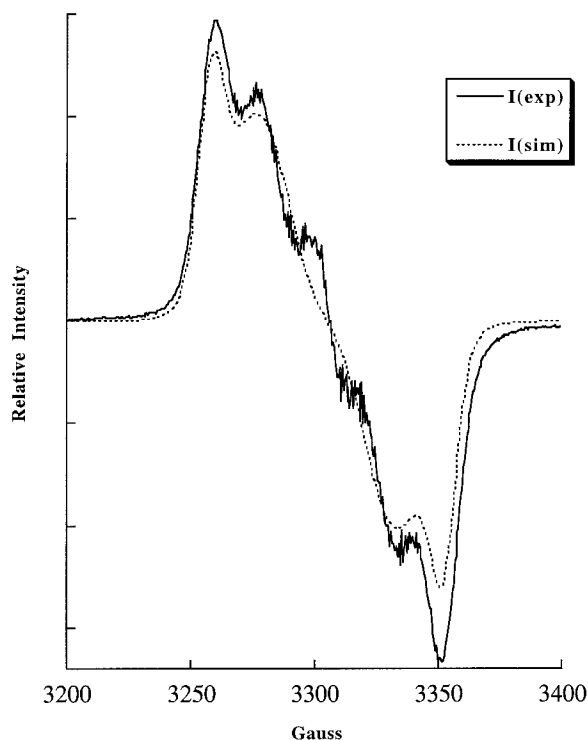
EPR Frozen Solutions. The spectra for compounds **4–7** in frozen solutions are consistent with those of randomly oriented triplets. In all compounds, a trace of a doublet impurity could be found. However, zero field splitting parameters (zfp) were still observed and simulated (Table 2).³³

The EPR spectra of frozen solutions of **5** and **6** are very similar. The simulated zfp³³ for **5** were $|D/hc| = 0.0043$

(33) Powder EPR spectra were simulated using WINEPR SimFonia, Shareware Version 1.25, Brüker Analytische Messtechnik GmbH, Copyright © 1994–1996.

Table 2. Zero Field Splitting Parameters and Curie Plot Results for Verdazyl Biradicals

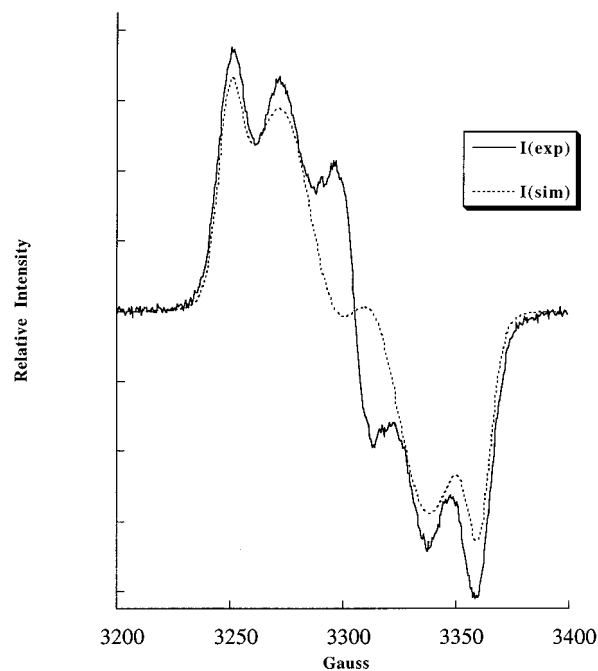
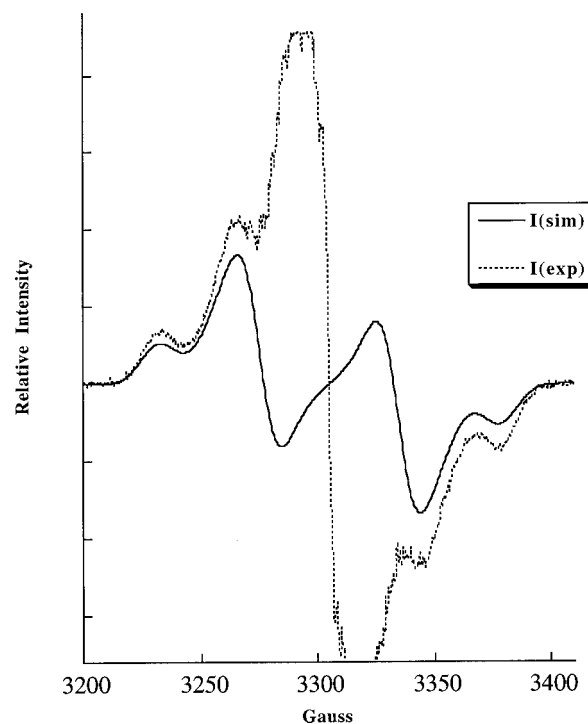
	$ D/hc $ (cm ⁻¹)	$ E/hc $ (cm ⁻¹)	Curie plot
1	0.038	0.0016	$J = 887$ cm ⁻¹¹⁰
7	0.018	0.0012	$J = 560$ cm ⁻¹
4	0.0063	0.0037	linear
5	0.0043	0.00042	linear
6	0.0051	0.00047	linear

**Figure 7.** EPR spectrum of **5** in a frozen, degassed THF solution.

cm⁻¹, $|E/hc| = 0.00042$ cm⁻¹ (Figure 7). The simulated zfp for **6** were $|D/hc| = 0.0051$ cm⁻¹ and $|E/hc| = 0.00047$ cm⁻¹ (Figure 8), indicating very little difference in the degree of electronic interaction between radical centers in compounds containing the *p*-phenylene and 2,5-thiophene spacers. Both compounds also gave linear Curie plots, indicating either a ground state triplet or a nearly degenerate ground state.²¹

The similarities in **5** and **6** are expected. Recall that cyclic voltammetry revealed one two-electron-oxidation wave, showing little interaction between the two unpaired electrons. Since the *D* value is inversely proportion to the average distance between the two electrons, the sites bearing electron density in these compounds must be farther apart. As such, lower levels of coupling would be expected than if they were more strongly interacting as in **4**, which had two one-electron oxidation waves. The zfp of **4** are larger than those of **5** and **6**. For **4**, $|D/hc| = 0.0063$ cm⁻¹, $|E/hc| = 0.00037$ cm⁻¹ (Figure 9). However, **4** also gave a linear Curie plot.

The spectrum of **7** in frozen chloroform is consistent with the hyperfine structure of a randomly oriented triplet³⁴ (Figure 7). The large featureless absorption in the middle of the spectrum is identical to that previously attributed to a doublet impurity.¹⁰ Zero field parameters

**Figure 8.** EPR spectrum of **6** in a frozen, degassed THF solution.**Figure 9.** EPR spectrum of **4** in a frozen, degassed THF solution.

$|D/hc|$ and $|E/hc|$ were determined to be 0.018 cm⁻¹ and 0.0012 cm⁻¹, respectively. The zero field parameters are smaller than those of the previously reported bisverdazyl **1** of $|D/hc| = 0.038$ cm⁻¹ and $|E/hc| = 0.0016$ cm⁻¹.¹⁰ The *D* value is smaller in **7** than in **1**, indicating a higher degree of delocalization of the unpaired electrons into the orbitals of the thione. Because the *D* parameter is a measure of the distance between the two unpaired electrons, and because the value for **7** is approximately half that of **1**, the unpaired electrons are likely localized further apart onto the two sulfur atoms, which is

(34) Wasserman, E.; Snyder, L. C.; Yager, W. A. *J. Chem. Phys.* **1964**, *41*, 1763.

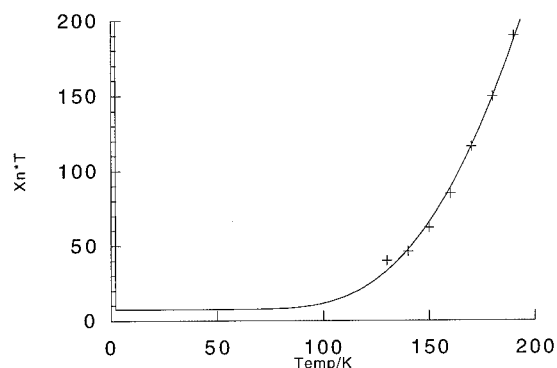


Figure 10. Dependence of the product of susceptibility and temperature ($\chi_N T$) on temperature (T) for **7**. The solid line is a best fit to the function $\chi_N T = P + ke^{-\Delta E/k_B T}$ with $\Delta E = 0.069$ eV, $k = 12200$, $p = 7.6$.

consistent with the cyclic voltammetry peak splitting. Thus, **7** has a peak splitting of about one-half of that of **1**.

Inspection of the half-field region of the spectrum of **7** reveals signals consistent with transitions between the $m_s = -1$ and $m_s = +1$ states of the triplet. The temperature dependence of this signal allows for the singlet–triplet energy separation J to be determined. The temperature dependence of $\chi_N T$ (where $\chi_N = I/I_{300}$, where I is the integrated signal intensity and I_{300} is the integrated signal intensity at 300 K), was determined from the EPR signal intensity for **7** (Figure 10). Fitting these data to eq 1¹⁰

$$\chi_N T = P + ke^{-\Delta E/k_B T} \quad (1)$$

gives a singlet–triplet energy gap of 560 cm^{-1} (0.069 eV). This value is lower than that found for **1**, where the activation energy has been determined to be 887 cm^{-1} (0.11 eV).¹⁰

Conclusions

Electronic coupling between the radical centers in substituted verdazyl biradicals is affected by substitution at the C_3 position. Aromatic spacers at C_3 in **4–6** decrease the magnitude of coupling between the two unpaired electrons, compared to **1**, as shown by cyclic voltammetry and EPR spectral measurements. This effect is illustrated in the observed electrochemistry, where two one-electron oxidation waves (to produce a dication) are observed for **1**, whereas a single two-electron oxidation wave is evident in **5** and **6**. Significant red shifts in the absorption spectra, however, indicate structural perturbation by these binding groups, although spectral broadening makes unambiguous assignment of the causes for these differences difficult.

Biradicals **4–6** all gave linear Curie plots with D values ranging from 0.0043 to 0.0063 cm^{-1} . A linear Curie plot confirms that each member of this family exists as a ground-state triplet or as a species with a degenerate triplet/singlet energy level.²¹

Replacement of oxygen at C_6 in **1** with sulfur in **7** does affect the electronic structure of the biradical. The absorption spectrum of **7** is red-shifted by about 50 nm from that of **1**. Electrochemical measurements indicate two one-electron oxidation waves in **7**, but scan reversal reveals only one return wave, suggesting an unstable

dication. Room-temperature EPR spectra of **7** are nearly identical to those for **1**, but $|D/hc|$ and $|E/hc|$ parameters derived from spectra of frozen solution suggest a higher degree of electronic delocalization in **7** than in **1**. Although biradical **7** is highly air sensitive, it displays a smaller singlet–triplet energy gap than the oxygen analogue **1**.

Experimental Section

General Methods. Phosgene (20% from Fluka) and methylhydrazine were used without further purification, producing 2,4-dimethylhydrazide.³⁵ This in turn was condensed with the dialdehyde of the spacer of interest to produce the corresponding tetrahydrazine. The tetrahydrazine was then oxidized with either potassium ferricyanide, tetraphenylhydrazine, or lead oxide to produce the desired bisverdazyl biradical.¹⁴

¹H and ¹³C NMR spectra were recorded on an NMR spectrometer at 300 and 75.5 MHz, respectively. X-band EPR spectra were recorded on a spectrometer fitted with a liquid helium cryostat. Powder EPR spectra were simulated using WINEPR SimFonia, Shareware version 1.25. Absorption spectra were recorded on a scanning spectrophotometer equipped with a near-infrared (IR) detector. Electrochemical measurements were carried out on a potentiostat using a Pt wire working electrode, a Pt coil auxiliary electrode, and a Ag/AgCl reference electrode. For each electrochemical experiment, the supporting electrolyte was 0.1 M NBu₄PF₆ in acetonitrile. The electrolyte had been recrystallized three times from absolute ethanol and dried under vacuum, and the solvent was purified according to previously described methods.³⁶ All other reagents were purchased from Aldrich and were used as received. Melting points were recorded on a capillary apparatus and are uncorrected.

Synthesis of 1,3-Bis(1,5-dimethyl-6-oxo-3-verdazyl)-benzene (4). To a solution of 0.42 g (3.1 mmol) of isophthalaldehyde in 5 mL of 100% ethanol, at 80 °C, was added 0.96 g (8.1 mmol) of 2,4-dimethylcarbonohydrazide. After heating for 5 min, a white precipitate had formed. The mixture was stored at 10 °C for 4 h and the white solid collected by filtration (63%). Mp: 181 °C (dec). ¹H NMR (DMSO-*d*₆): δ 7.72 (1 H, s), 7.48–7.36 (3 H, m), 5.68 (4 H, d), 4.90 (2 H, t), 2.94 (12 H, s). ¹³C NMR (DMSO-*d*₆): 154.5, 136.8, 128.1, 126.5, 126.1, 68.6, and 37.6 ppm. HRMS (CI): (*m/z*) C₁₄H₂₀N₈O₂ (M + H)⁺ calcd 335.1944, found 335.1938.

Into a small vial, 102.5 mg (0.306 mmol) of 1,3-bis(1,5-dimethylhexahydro-6-oxo-1,2,4,5-tetrazin-3-yl)benzene and 732.6 mg (3.27 mmol) of lead oxide in 10 mL of dry THF were stirred for 24 h under inert conditions. The lead oxide was removed by filtering an EPR sample through a 0.2 μm Teflon syringe filter, yielding a red solution. HRMS (CI): (*m/z*) C₁₄H₁₆N₈O₂ (M + H)⁺ calcd 329.147, found 329.147.

Synthesis of 1,4-Bis(1,5-dimethyl-6-oxo-3-verdazyl)-benzene (5). In a round-bottom flask was placed 100 mg (0.31 mmol) of 1,4-bis(1,5-dimethylhexahydro-6-oxo-1,2,4,5-tetrazin-3-yl)benzene²⁹ in 6 mL of water. Na₂CO₃ (3 mL, 2 N) was added together with 600 mg (1.8 mmol) of K₃Fe(CN)₆ in 5 mL of water. The solution was stirred for 4 h and was then extracted with CH₂Cl₂. The solvent was removed under vacuum. The product (50 mg, 0.15 mmol, 48%) was collected as a red solid. Mp: 250 °C (dec). UV–vis (CH₃CN): λ_{max} nm (log ϵ): 415 (3.17), 277 (4.48), 200 (4.28). HRMS (CI): (*m/z*) C₁₄H₁₆N₈O₂ (M + H)⁺ calcd 329.3531, found 329.1487. LRMS (CI⁺): 329 (49%).

Synthesis of 2,5-Bis(1,5-dimethyl-6-oxo-3-verdazyl)-thiophene (6). To a solution of 1.1 g (8.9 mmol) of 2,4-dimethylcarbonohydrazide in 10 mL of ethanol was added 0.50 g (3.6 mmol) of thiophenedicarboxaldehyde. The solution was

(35) Raphaelian, L.; Hooks, H.; Ottmann, G. *Angew. Chem., Int. Ed. Engl.* **1967**, *6*, 363.

(36) Knorr, A. *Funktionalisierte Fluoreszenzfarbstoffe auf Anthracen- und Pyrenbasis*; Knorr, A., Ed.; University of Regensburg: Regensburg, 1995.

heated to reflux for 45 min and then cooled to room temperature. A solid formed upon cooling which was separated by filtration, yielding 0.84 g (69%) as a white powder. Mp: 242–3 °C. ¹H NMR (DMSO-*d*₆): δ 6.96 (s, 2 H), 5.83 (d, 4 H, *J* = 5.7 Hz), 5.07 (t, 2 H, *J* = 5.4 Hz), 2.92 (s, 12 H). ¹³C NMR (DMSO-*d*₆): 154.0, 140.9, 125.5, 65.5, and 37.9 ppm. UV–vis (DMSO): λ_{max} nm (log ε): 318 (3.05). HRMS (CI): (*m/z*) C₁₂H₂₀N₈O₂S (M + H)⁺ calcd 341.42, found 341.151.

To a solution of 100 mg (0.30 mmol) of 2,5-bis(1,5-dimethylhexahydro-6-oxo-1,2,4,5-tetrazin-3-yl)thiophene in 7 mL of water was added 600 mg of K₃Fe(CN)₆ (1.8 mmol) in 6 mL of water and 3 mL of 2N Na₂CO₃. The solution was stirred for approximately 6 h, and the resulting brown solution was extracted with CHCl₃. The solvent was removed under vacuum and the resulting yellow-brown solid collected by filtration (48 mg, 0.14 mmol). Mp: 245 °C (dec). UV–vis (CH₃CN): λ_{max} nm (log ε): 357 (4.70, sh), 343 (4.78, sh), 317 (4.92), 300 (4.98, sh), 194 (5.02). HRMS (CI): (*m/z*) C₁₂H₁₄N₈O₂S (M + H)⁺ calcd 335.3773, found 335.103. LRMS (CI⁺): 335 (100%).

Synthesis of 1,1',5,5'-Tetramethyl-6,6'-dithio-3,3'-biverdazyl (7). A solution of 0.67 g (5.0 mmol) of 2,4-dimethylthiohydrazide was combined with 0.60 g (2.3 mmol) of glyoxal sodium bisulfate addition compound in 15 mL of distilled water, and the resulting solution was heated to reflux for 2 h.

The solution was cooled to room temperature and the product collected by filtration, yielding 0.51 g (1.7 mmol, 34%) of product as a brownish yellow powder. Mp: 271 °C. ¹H NMR (DMSO-*d*₆): δ 5.60 (d, 4 H, *J* = 6.1 Hz), 3.82 (t, 2 H, *J* = 6.6 Hz), 3.31 (s, 12 H). ¹³C NMR (DMSO-*d*₆): 173.7, 66.0, 43.7 ppm. HRMS (CI): (*m/z*) C₈H₁₈N₈S₂ (M + H)⁺ calcd 291.43, found 291.12. LRMS (CI⁺): 291 (89%).

A vacuum-sealed solution of 0.024 g (0.087 mmol) of 2,2',3,3',4,4',5,5'-octahydro-1,1',5,5'-tetramethyl-3,3'-bis-1,2,4,5-tetrazin-6,6'-thione and 0.072 g (0.25 mmol) of tetraphenylhydrazine in 2 mL of degassed CHCl₃ was heated in an oil bath at 330 K for 48 h, turning first green and then dark purple. UV–vis (CH₃CN) λ_{max} (log ε): 284 (3.56).

Acknowledgment. This work was supported by the National Science Foundation and the Robert A. Welch Foundation. We are grateful to Dr. David Brook for helpful suggestions regarding the synthesis and spectral interpretations included here. We would like to thank Dr. David Shultz for his useful discussions and the use of his equipment.

JO990962S